Locally resolved isotropic and anisotropic ^{13}C Knight shifts in the organic conductor (fluoranthenyl)$_2X$ ($X = AsF_6$, PF_6)

D. Köngeter* and M. Mehring
2. Physikalisches Institut, Universität Stuttgart, Pfaffenwaldring 57, D-7000 Stuttgart 80, Federal Republic of Germany
(Received 13 June 1988; revised manuscript received 14 November 1988)

^{13}C Knight-shift tensors including both the isotropic and anisotropic parts of the organic conductors (fluoranthenyl)$_2X$ with $X = AsF_6$ or PF_6 have been obtained by NMR experiments on powdered samples and on single crystals. It is found that the anisotropic part of the Knight shift yields a more direct access to the local p_z spin-density distribution of the conduction-electron band than the isotropic part.

I. INTRODUCTION

The radical cation salts of fluoranthene (abbreviated in the following by FA) can serve as model compounds for a large class of organic conductors. Their structure consists of stacks of FA molecules accompanied by stacks of inorganic anions (AsF_6^- or PF_6^-).[1] The crystal structure is shown in Fig. 1 together with the numbering of the carbon atoms on the FA molecule used in this paper.

These crystals show strong one-dimensional character as is suggested by the crystal structure. This is reflected in the anisotropic conductivity[2] and in the highly anisotropic spin-diffusion constant,[3] which is 3 orders of magnitude larger in the stacking direction than perpendicular to it. A number of different magnetic resonance experiments have revealed the conductivity to take place on the organic stack only.[4,5] Proton spin-lattice relaxation on the FA protons showed strong relaxation, whereas the ^{19}F relaxation of the anions was observed to be very weak.[4] Overhauser shift measurements demonstrated unequivocally that the FA protons are strongly hyperfine coupled to the conduction electrons.[5]

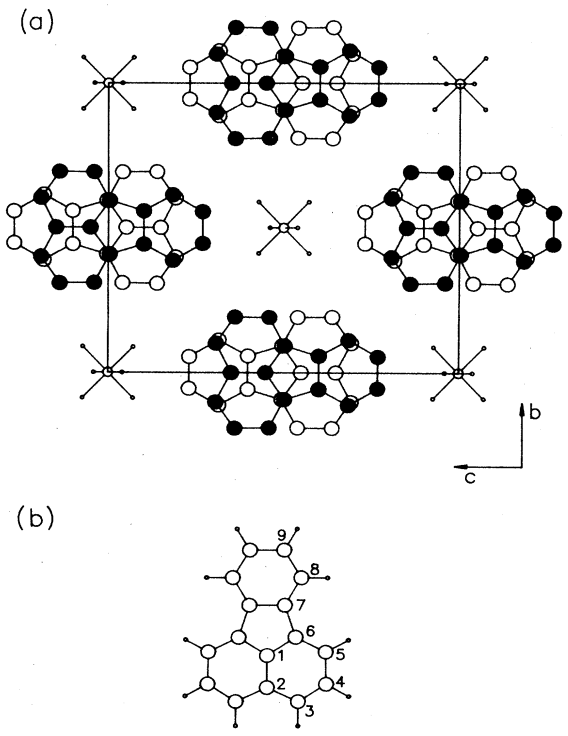

FIG. 1. (a) Crystal structure of fluoranthene radical cation salts projected along the stacking axis c. (b) Single fluoranthene molecule with the numbering of the different carbon sites on the molecule used in this paper.

This was also demonstrated by the first report on locally resolved ^{13}C Knight shifts in organic conductors.[6] The technique of high-resolution NMR in the solid state applied to ^{13}C (Refs. 6 and 7) and protons[7,8] has proven to be very useful for obtaining a locally resolved spin-density map of the conduction band. Similar experiments have been reported on powdered samples of other organic conductors,[9,10] whereas the proton experiments obviously led to information only about the sites bonded to protons, the hitherto existing ^{13}C data of powdered samples gave only indirect hints to the local p_z-spin density.[7,11] Additional difficulties in these experiments arise from the assignment of the NMR lines to the different sites and from the separation of the Knight shift from the chemical shift. In order to solve the latter problem, we have performed temperature-dependent ^{13}C Knight-shift measurements in the metallic regime of (FA)$_2X$ combined with high-resolution techniques. This procedure was first applied to the organic conductor $(TMTSF)_2ReO_4$ by Bernier and co-workers[12,13] and will be discussed in more detail below.

We report here in particular on ^{13}C Knight-shift experiments on single crystals of $(FA)_2PF_6$ which could solve some of the remaining problems: We have determined on the one hand the dipolar parts of the hyperfine interaction with the conduction electrons which gave a more direct access to the local p_z spin densities than its isotropic parts. On the other hand, this supplied an assignment of the NMR lines to the different carbon sites by the aid of the anisotropy of the ^{13}C-H dipolar interaction. Whereas the anisotropy of the proton Knight shifts of these salts has been published before,[8] we believe that we present here the first example of the fully resolved ^{13}C Knight-shift anisotropy in organic conductors. Earlier reports on anisotropic behavior of the ^{13}C Knight shift used sideband analysis of magic-angle sample spinning

spectra of β-(BEDT-TTF)$_2I_3$ (Ref. 14) or dynamic nuclear polarization in single crystals of $(FA)_2PF_6$ (Ref. 15). In these reports, however, only a hint at the Knight-shift anisotropies was supplied and no complete determination of the locally resolved Knight-shift tensors was possible. Likewise, Overhauser shift experiments on $(FA)_2PF_6$ showed important anisotropic contributions to the ^{13}C hyperfine interactions,[16] but up to now no local resolution was possible.

II. CHEMICAL-SHIFT AND KNIGHT-SHIFT TENSOR

The nuclear-magnetic-resonance line is always shifted with respect to the bare Larmor frequency $\omega_0=\gamma_n B_0$, where γ_n is the gyromagnetic ratio of the nucleus and B_0 is the applied static magnetic field. The shift $\Delta\omega$ of the resonance line of a particular nucleus is due to the averaged magnetic local field caused by the surrounding electrons. In diamagnetic substances this shift is called the "chemical shift,"[17] whereas in metals an additional shift called the "Knight shift"[18] after its discoverer is observed, which is caused by the averaged hyperfine field of the conduction electrons.

Since the nomenclature of chemical shifts and Knight shifts varies in the literature and the chemical-shift tensor is usually ignored in ordinary metals, we summarize briefly the essential expressions for the convenience of the reader. The relative shift $\delta=\Delta\omega/\omega_0$ of the resonance line can be represented by the general-shift Hamiltonian

$$\mathcal{H}_S=-\hbar\gamma_n\mathbf{I}\cdot\tilde{\delta}\cdot\mathbf{B}_0 , \tag{1}$$

where the shift tensor $\tilde{\delta}$ can be separated into an isotropic and anisotropic part

$$\tilde{\delta}=\delta_{\rm iso}\tilde{\mathbf{E}}+\tilde{\delta}_{\rm ani} , \tag{2}$$

with unit matrix $\tilde{\mathbf{E}}$. For usual chemical and Knight shifts all elements of the 3×3-shift matrix are much smaller than unity, i.e., only the secular part of the shift Hamiltonian

$$\mathcal{H}_S=-\hbar\gamma_n B_0\delta_{zz}I_z \tag{3}$$

needs to be considered. Only the symmetric part of the shift tensor contributes to the observed relative resonance shift δ_{zz}, which can be expressed by the three principal elements $(\delta_{11},\delta_{22},\delta_{33})$ as

$$\delta_{zz}=\delta_{11}\cos^2\alpha\sin^2\beta+\delta_{22}\sin^2\alpha\sin^2\beta+\delta_{33}\cos^2\beta , \tag{4}$$

where (α,β) are the Euler angles of the magnetic field with respect to the principle-axis system (1,2,3). Rotation plots of the resonance shift therefore allow us to determine the principal elements and the principle-axis system of the shift tensor. For completeness we note that

$$\delta_{\rm iso}=(\delta_{11}+\delta_{22}+\delta_{33})/3 .$$

The total shift tensor $\tilde{\delta}$ can, in metals, be separated into two parts, namely (i) chemical shift and (ii) Knight shift.

(i) *Chemical shift.* Let us suppose that the chemical-shift tensor is caused by all the electrons in the molecule or solid except the conduction electrons. The chemical-shift tensor can again be separated into two parts, namely the "diamagnetic" part δ^d_{ab} and the "paramagnetic" part δ^p_{ab}, with $a,b=x,y,z$,

$$\delta^d_{ab}=-\frac{2m\beta_e^2}{\hbar^2}\left\langle 0\left|\sum_i\frac{r_i^2\Delta_{ab}-a_ib_i}{r_i^3}\right|0\right\rangle , \tag{5a}$$

and

$$\delta^p_{ab}=\frac{2\beta_e^2}{\hbar^2}\sum_{n>0}(E_n-E_0)^{-1}\times\left[\left\langle 0\left|\sum_i r_i^{-3}l_{ia}\right|n\right\rangle\langle n|L_b|0\rangle+\text{c.c.}\right] , \tag{5b}$$

where $|0\rangle$ is the ground state and $|n\rangle$ are the exited states. β_e is the Bohr magneton, Δ_{ab} is the Kronecker delta here and in the following equations, and $a_i,b_i=x_i,y_i,z_i$ are the components of the electron coordinate $\mathbf{r}_i$. The sum is to be taken over all exited electron states. Note that in the paramagnetic term the total orbital angular momentum with operator $\mathbf{L}=\sum_i l_i$ is "partially dequenched" by B_0. In diamagnetic molecules the chemical shift is the only mechanism which gives rise to the resonance shift. It is dominated by the molecular orbitals (MO) of the individual molecule even in the solid state. This chemical shift is also the dominant shift mechanism in organic conductors. It usually leads to large shift anisotropies. Due to the conduction electrons in organic conductors there is an additional shift, i.e., the Knight shift.

(ii) *The Knight shift.* Before we discuss the Knight shift due to the spin paramagnetism of the conduction electrons in more detail, we want to discuss what is usually termed the "Van Vleck orbital Knight shift." It can be derived from essentially the same expression as Eq. (5b) if the conduction band MO is included. A simple estimate of the orbital Knight-shift contribution due to a tight-binding–type conduction band leads to the expression[19]

$$K_{\rm orb}\simeq\frac{(N-n)n}{N\Delta E}\beta_e^2\langle r^{-3}\rangle , \tag{6}$$

where N is the total number of conduction electrons, n is the number of occupied states in the conduction band, ΔE is the effective bandwidth, and where the average over the electron coordinates has to be taken over the atomic/molecular orbital from which the band is constructed, e.g., in organic conductors, this is usually a p-wave function. Note that $K_{\rm orb}$ does not depend on the density of states at the Fermi level. Equation (7) is only valid though in three-dimensional solids. In one-dimensional solids, however, the orbital contribution vanishes as can be seen from Eq. (5b). However, real organic conductors are at best quasi one dimensional, i.e., the ratio of the transverse to the longitudinal transfer integrals $t_\perp/t_\parallel$ may be small [$<10^{-2}$ in $(FA)_2X$] in organic conductors but certainly does not vanish. It is therefore expected that the orbital contribution to the Knight shift will be scaled by this ratio of transfer integrals. In the conductor discussed here, namely $(FA)_2X$, this ratio is

rather small and the orbital contribution can be neglected.

All hyperfine interactions (including contact, dipolar, s like, and core polarization, etc.) of the conduction electrons with the nuclei in the sample can be summarized under the hyperfine tensor $\tilde{A}$. As in the chemical-shift case (see related discussion) we consider only the secular part of the hyperfine Hamiltonian

$$\mathcal{H}_{IS}=\hbar A_{zz} I_Z S_Z \ . \tag{7}$$

Again, a separation into an isotropic part $a_{\rm iso}$ and an anistropic but traceless part $\tilde{A}'$ is possible. The orientational dependence of A_{zz} is similar to Eq. (4) and the principal elements A_{11}, A_{22}, A_{33} can be determined from an orientation plot in the magnetic field.

Due to the rapid motion of the conduction electrons (with Fermi velocity v_F) only an average of their spin component is "seen" by the nuclei. The total Hamiltonian of the spin-paramagnetic Knight shift can be expressed as

$$\mathcal{H}_K=-K_{ZZ}\hbar\omega_0 I_Z \ , \tag{8a}$$

with

$$K_{ZZ}=\frac{\chi_s}{N} A_{ZZ}/(g_e\beta_e\gamma_n) \ . \tag{8b}$$

The electron-spin susceptibility χ_s is related to the density of states $N(E_F)$ at the Fermi level in the random-phase approximation by

$$\chi_S=\chi_p/[1-UN(E_F)] \ , \tag{9a}$$

where the Hubbard U takes care of electron-electron correlations and the Pauli susceptibility in a tight-binding approximation can be expressed as

$$\chi_p=\tfrac{1}{2}(g_e\beta_e)^2 N(E_F) \ . \tag{9b}$$

The enhancement of χ_S due to electron-electron correlation [Eq. (9a)] leads to a proportionally enhanced Knight shift.

K_{ZZ} according to Eq. (8b) contains the full tensorial character (symmetric part only) of the hyperfine interaction and is related to the principal elements K_{11}, K_{22}, and K_{33} equivalent to Eq. (4). The connection between the hyperfine tensor elements A_{aa} and the Knight-shift tensor elements K_{aa} $(a=1,2,3)$ is given by Eq. (8b). The Knight-shift tensor can also be separated into an isotropic and a traceless anisotropic part. We will discuss both parts separately in the following.

The isotropic Knight shift $K_{\rm iso}=(K_{11}+K_{22}+K_{33})/3$ is directly related to the isotropic hyperfine interaction $a_{\rm iso}$ by Eq. (10). In ordinary metals this is the dominant contribution to the Knight shift. For s-like electron states this leads to the Fermi contact term. In organic conductors, however, mostly p-like orbitals set up the conduction band, which have a node at the carbon nuclear position. So the Fermi contact contribution is usually negligibly small in these materials. In this case the experimentally observed isotropic part of the hyperfine interaction is due to the "core polarization" of the $2s$ and $1s$ orbitals. Pople and Beveridge[20] demonstrated a linear behavior between $2s$ spin densities at carbon sites and the experimentally observed ^{13}C isotropic hyperfine interactions in organic radicals (see also Ref. 11). This mechanism will be the dominant one for the isotropic Knight shift in organic conductors.

Both contributions to the isotropic hyperfine interaction, namely Fermi contact and core polarization, can be finally represented by

$$a_{\rm iso}=\frac{8\pi}{3} g_e\beta_e\gamma_n\rho_S(o) \ , \tag{10}$$

where $\rho_S(o)$ is the spin density at the atomic s orbitals, induced by conduction electrons in other orbitals at the particular site or in orbitals on neighboring sites. This can be cast into the semiempirical Karplus-Fraenkel[11] relation for the isotropic hyperfine interaction $a_j/2\pi$ (in MHz) at position j:

$$a_j/2\pi=Q\rho_j+\sum_i Q_n\rho_i \ , \tag{11}$$

with the values $Q=100$ MHz for secondary carbon atoms, $Q=85$ MHz for tertiary carbon atoms, and $Q_n=-39$ MHz. The ρ_j are the spin densities in the p_z orbitals at site j; the sum runs over the two or three carbon neighbors, respectively. The cases where this simple formula applies are, however, limited. Problems arise in particular when the spin density at neighboring sites becomes dominant and when the difference between on-site and neighboring-site contributions leads to small hyperfine interactions. The Karplus-Fraenkel relation should therefore be applied "*cum grano salis.*"

Next, we discuss the anisotropy of the ^{13}C Knight shift, which arises from the anisotropic hyperfine interaction due to electron-nuclear dipolar interaction. In a previous publication we have reported on the proton Knight-shift tensor.[8] The anisotropic part of the hyperfine interaction Hamiltonian can be represented by the single-particle electron spin density $\rho_S(\mathbf{r})$ at position $\mathbf{r}$:

$$A'_{ab}=g_e\beta_e\gamma_n\int r^{-5}(3r_a r_b-r^2\Delta_{ab})\rho_S(\mathbf{r})d^3r \ . \tag{12}$$

The strong distance dependence of this anisotropic hyperfine interaction makes it a suitable parameter for monitoring the on-site spin density.

In order to determine the Knight-shift tensor experimentally one has to subtract the chemical-shift tensor from the measured data. In the past[6,7] we have used neutral fluoranthene in solution[21] as reference chemical-shift spectra. In the cationic state of the fluoranthene molecule in the organic conductor $(FA)_2X$, the chemical shift may be altered with respect to the neutral molecule. It seems, therefore, appropriate to look for a more direct way to separate the paramagnetic Knight-shift contribution from the chemical shift. Since the paramagnetic Knight shift is, according to Eq. (8b) directly proportional to the spin susceptibility of the conduction electrons, there are basically two different ways to utilize this relation.

In the first approach one saturates the electron spins

which affects the spin susceptibility directly in a controllable way by microwave absorption. Experiments along these lines were proposed some time ago[22] and have been performed recently.[15,23] In this paper we have used the second approach, i.e., the temperature dependence of the paramagnetic spin susceptibility which has been measured recently quite accurately.[24,25] This will be discussed in more detail in the following sections.

III. EXPERIMENTAL RESULTS

The samples of $(FA)_2AsF_6$ and $(FA)_2PF_6$ were grown electrochemically as described by Kröhnke *et al.*[26] The NMR experiments were performed at a ^{13}C Larmor frequency of 46 MHz and the corresponding proton Larmor frequency of 181 MHz.

Standard solid-state high-resolution NMR techniques, such as cross polarization including magic-angle sample spinning (MAS) in the case of powders were applied.[27] The MAS spectrum is shown in Fig. 2 on the right-hand side. Eight lines labeled *a*–*h* can be distinguished. The line *g* is a superposition of two lines and the unmarked lines were identified as spinning sidebands. Line *h* was not observed in earlier work[6,7] because it is easily hidden by one of the spinning sidebands. No difference was observed between the spectra of $(FA)_2AsF_6$ and $(FA)_2PF_6$.

In order to separate the Knight shift from the chemical shift we have peformed temperature-dependent magic-angle-spinning experiments from room temperature down to the metal-insulator phase transition at about 180 K. These experiments were performed on a MSL200 spectrometer at the Bruker company in Karlsruhe. The cooling of the spinning sample was achieved by a cold nitrogen stream acting as a gas bearing. The middle part of Fig. 2 shows the development of the spectrum with decreasing temperature. At the left-hand side we sketched

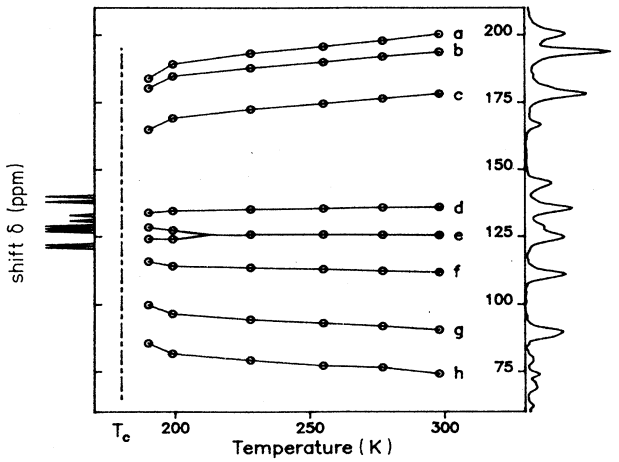

FIG. 2. ^{13}C-cross polarization/magic-angle spinning spectra of $(FA)_2AsF_6$ vs temperature. The right-hand side shows a room temperature spectrum, on the left-hand side we have sketched the ^{13}C spectrum of neutral fluoranthene in solution. The unmarked lines on the rightband spectrum are spining sidebands. All shift values are with respect to TMS (tetramethylsilane).

as a possible reference the resolved chemical-shift spectrum of neutral fluoranthene in solution, which is known from the literature.[20] The spectra of the radical cation salt obviously converge to the solution spectrum. The splitting of line *e* may be caused by a structural phase transition.[1]

Assuming that the spin susceptibility is the only temperature-dependent parameter in the Knight shift, one can evaluate from the slope ratios in Fig. 2 the ratios of the individual Knight shifts with respect to each other. This procedure makes no use of the functional behavior of the spin susceptibility. We prefer this procedure to the one where the Knight shift is plotted versus the spin susceptibility because the latter did not give the expected linear behavior. The reason for this might be the fact that only the spin susceptibility of Refs. 24 and 25 was available to us, which was, of course, determined for different samples. It is conceivable that our samples might have had a slightly different temperature dependence of the spin susceptibility. On the other hand, neutral fluoranthene can only serve as a crude chemical-shift reference, since the molecules are in the cationic state in this type of organic conductor and it is expected that their chemical-shift tensor is different. We therefore feel more confident with the procedure outlined here. It is, anyway, the only procedure which can be applied when precise spin susceptibility data are not available.

Absolute Knight shifts were obtained by taking the chemical-shift value at position 7 of dissolved fluoranthene as the appropriate reference for line *b*, anticipating the line assignment used earlier for this line and discussed below.[7] Any error in the *absolute* value does not drastically affect the spin-density distribution over the molecule, however. The numeric values are collected in Table I, which also contains the line assignments to be discussed later. For comparison we have added the chemical-shift data of neutral fluoranthene in solution[21] which was used in an earlier report[7] as a Knight-shift reference. We do, however, believe that the Knight shift obtained from the temperature dependence is more reliable than subtracting the chemical shift from the solution spectrum. Table I, however, also demonstrates that there is not much difference between the Knight shifts determined by these two different approaches. Finally, we mention that the reference problem was recently approached by saturating the conduction-electron spins by microwave irradiation combined with magic-angle spinning.[23] There the Knight shift is directly affected and varies with the microwave field, whereas the chemical shift is independent of the microwave power. This allows a separation of Knight and chemical shifts.[23] The slight discrepancies between the Knight shifts obtained by these different methods are not yet fully understood.

Orientation dependent experiments were performed on single crystals of $(FA)_2PF_6$ of typical size $5\times1\times1$ mm^3. In contrast to the magic-angle-spinning experiments, where the ^{13}C-^{19}F dipole-dipole interaction is averaged out by sample rotation, in single-crystal measurements the ^{19}F spins must be decoupled by applying a strong rf field at their Larmor frequency. The effect of this triple-resonance experiment is shown in Fig. 3. Without

TABLE I. Experimental results of ^{13}C Knight-shift experiments on powdered samples (δ_{iso},K_{iso}) and on single crystals together with T_1 data. The δ values denote the entire shift (chemical shift plus Knight shift) in ppm vs TMS. The shift-tensor orientation in the fluoranthene molecule is given by the angle (column 7) between its first principal axis and the molecular mirror plane; the third principal axis is always oriented perpendicular to the molecular plane. The Knight-shift values were derived as described in the text.

Site	δ_{iso} (MAS)	δ_{iso} (FA liquid)	δ_{11}	δ_{22}	δ_{33}	Orient.	K_{iso}	K_{33} (ppm)	T_1 (ms)
1	88.6	132.9	161.3	153.0	−49.0	90.0°	−35.7	−40	430
2	74.2	130.9	157.2	150.8	−87.0	90.0°	−48.2	−78	410
3	200.3	127.4	243.5	165.7	194.0	12.0°	64.5	184	80
4	111.7	128.8	197.5	124.5	14.0	59.6°	−18.2	4	1200
5	135.9	121.0	201.9	146.0	62.0	58.2°	7.2	70	500
6	193.8	137.6	223.4	172.1	192.0	0.0°	56.2	182	105
7	90.5	140.1	181.9	121.0	−34.0	28.7°	−35.9	−48	430
8	178.1	122.3	226.6	156.5	157.0	86.0°	54.5	165	120
9	125.5	128.4	212.0	133.1	32.0	24.8°	−3.7	36	1500

fluorine decoupling the necessary resolution can certainly not be achieved.

Figure 4 shows the orientational dependence of the spectra by rotation about an axis along the stacking direction, i.e., the magnetic field was always oriented perpendicular to the stacking direction. From the molecular symmetry and the symmetry of the $(FA)_2X$-type crystals it is expected that one principle axis of the Knight- as well as the chemical-shift tensor is oriented perpendicular to the molecular plane. We have therefore performed measurements with the magnetic field oriented parallel to the stacking direction. In order to improve the signal-to-noise ratio we have assembled several small needle like crystals parallel with respect to each other. The procedure was justified *"a posteriori"* in the sense that these data combined with the data from Fig. 4 resulted in the correct isotropic-shift values determined from magic-angle-spinning spectra. Moreover, the analysis of the

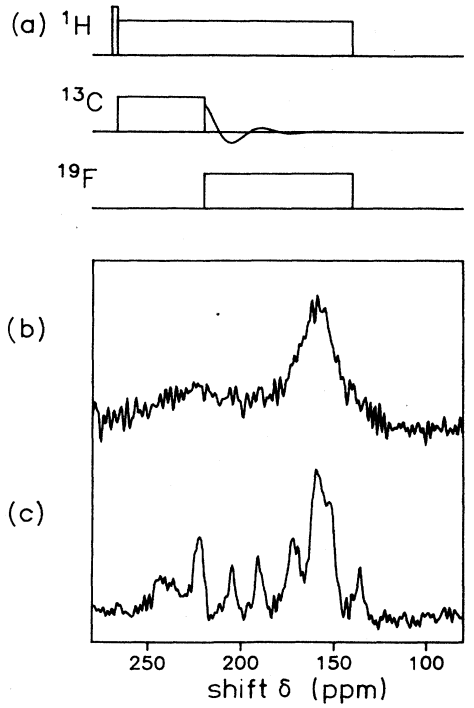

FIG. 3. Pulse sequence (a) and ^{13}C spectra in a $(FA)_2PF_6$ single crystal without (b) and with (c) ^{19}F decoupling.

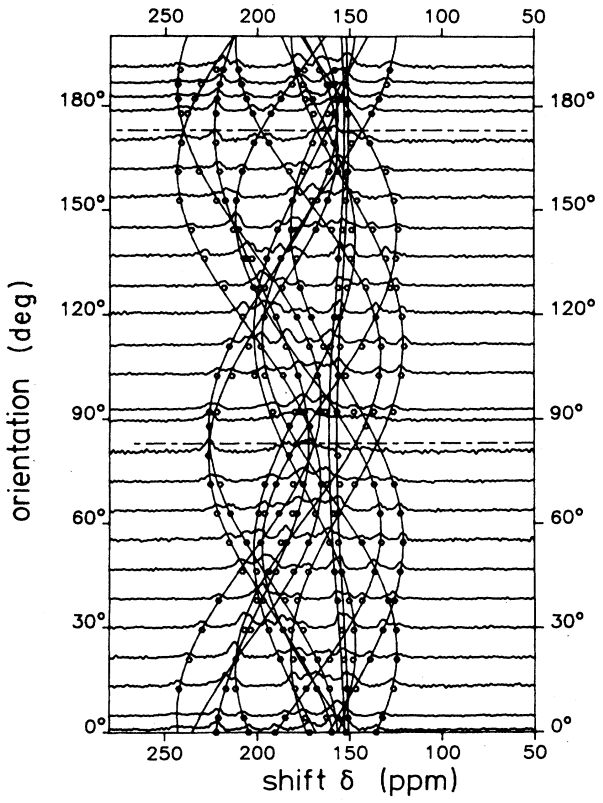

FIG. 4. Single-crystal spectra of $(FA)_2PF_6$ with rotation about an axis along the stacking direction, i.e., the magnetic field lies in the plane of the fluoranthene molecules. The dashed lines indicate mirror planes of the spectra. This is expected because of the mirror symmetry of the crystal structure. At 173° the static field direction points along mirror plane. Shift values are with respect to TMS.

spinning sideband intensities according to the Herzfeld-Berger procedure[28] gave similar principal axis values, although not as reliable as the single-crystal measurements discussed here.

The results are presented in Fig. 5 in a pictorial way together with the chemical-shift tensor of solid benzene at 14 K (Ref. 29) which serves as an exemplaric aromatic chemical-shift tensor reference. The numeric values of the shift tensor together with the tensor orientation are listed in Table I. Most orientations coincide with the expected orientation of chemical-shift tensors in aromatic solids, where the first principal axis (the least shielded direction) is oriented along the C—H bond and where the third princpal axis is perpendicular to the molecular plane.[30] A considerable deviation for site 3 is probably due to a tilted bond.

For unambiguous line assignment of the different carbon positions on the fluoranthene molecule we have performed "delayed decoupling" experiments on single crystals.[31] The dipole-dipole interaction between ^{13}C and the neighboring protons serves here as a "direction finder." The appropriate pulse scheme is shown in Fig. 6(a). After cross polarization, a variable delay time τ where dipolar interaction is present is inserted, before proton decoupling is applied. The data acquisition, however, starts independently from the delay time in order to avoid phase distortions. In contrast to delayed decoupling experiments on $(FA)_2X$ powder samples under magic-angle spinning[6] where only proton bonded carbons were distinguished from nonproton bonded carbons, we have utilized here the full orientational dependence of the dipolar interaction which leads to an unequivocal line assignment.

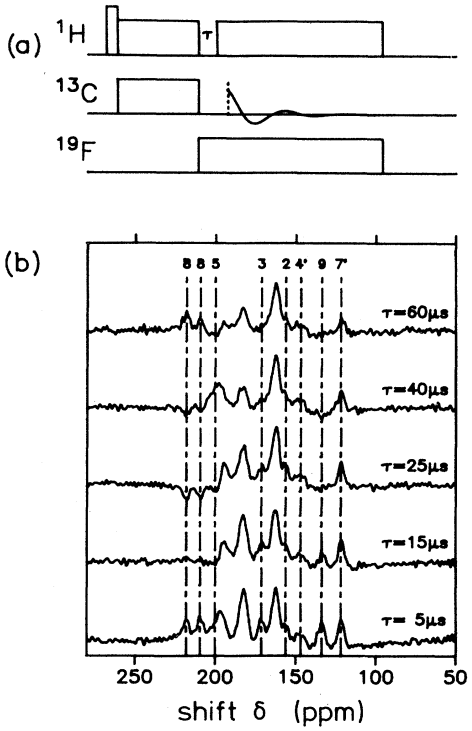

FIG. 6. Delayed decoupling experiment on a single crystal of $(FA)_2PF_6$ for assignment of the resonance lines, (a) pulse scheme, (b) set of spectra for different delays. The spectra to the orientation of 58° in Fig. 4. The numbers refer to Fig. 1(b); primed numbers indicate positions on the left side of the mirror plane.

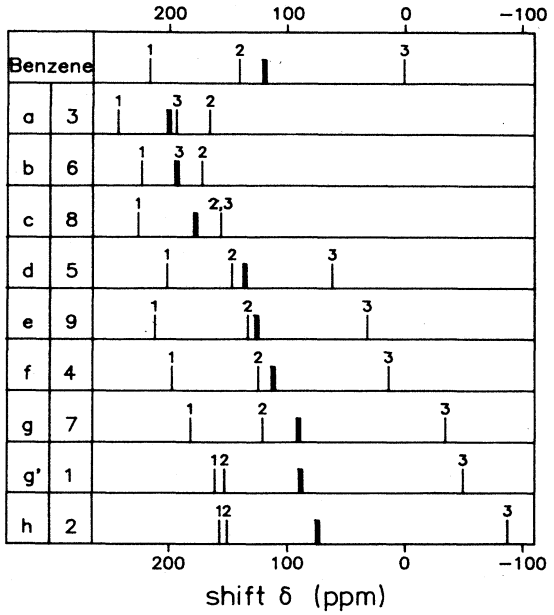

FIG. 5. Graphical representation of the tensor principal axes of the entire shift (chemical shift plus Knight shift). Thick lines denote the positions of the isotropic values. The left column gives the assignment using the numbering in Fig. 1(b). The chemical-shift tensor of benzene serves as an exemplaric chemical-shift reference. Shift values are with respect to TMS.

Figure 6(b) shows the spectra for a specific crystal orientation. Note, that line 4', for example, hardly decays in this orientation, although this carbon is bonded to a proton. Experiments of this sort were carried out for many different orientations, to allow the assignment of all shift tensors to the appropriate sites. This assignment was used in Table I and the left-hand side of Fig. 5. A slight uncertainty, though, remains for sites 4 and 5 corresponding to lines *d* and *f* because of their special orientation with respect to the molecular mirror plane. Therefore, we had to consider the different distortions of the "aromatic character" at these sites by the 5-ring structure.

Unfortunately, the ^{13}C chemical-shift tensor in neutral fluoranthene is not known accurately enough to serve as a reference for obtaining the Knight-shift tensor, as in the isotropic case. As mentioned above, the values for solid benzene may be taken as a guide line. We used here the analysis of the temperature dependence of the line shifts in the metallic regime. The K_{33} component of the different Knight-shift tensors were measured at various temperatures by orienting the magnetic field parallel to the stacking axis.[32] With the help of the isotropic part the average of K_{11} and K_{22} can be determined. As in the case of the isotropic Knight shift, only the Knight-shift ratios (component K_{33} only) of the different lines are ob-

tained from the temperature dependence. Again, the appropriate reference has to be assumed for at least one site.

In principle, one could do without such a reference by using the technique of Knight-shift saturation as was mentioned above. This technique was applied in a recent single-crystal investigation.[15] However, only the effect was demonstrated, but no information on the Knight-shift nor on the chemical-shift tensor was obtained.

We estimate the accuracy for our shift values δ_{ii} (chemical shift plus Knight shift) to about ± 0.5 ppm for δ_{iso}, ± 1 ppm for δ_{11} and δ_{22}, and to ± 2 ppm for δ_{33}. The orientation of the principal axis with respect to the molecular mirror plane was determined to an accuracy of about $\pm 0.5°$. The error of the K_{iso} values is in general about ± 1.5 ppm, not taking into account any error in the absolute value of the Knight shift of the reference line *b*. The absolute error for K_{33} is estimated to about ± 10 ppm, because of the uncertainty of the correct reference shift.

Finally, we report on some ^{13}C spin-lattice relaxation time (T_1) measurements which extend earlier published data.[6] Our values are summarized in Table I. Their accuracies are estimated to about $\pm 10-15\,\%$. Since the relaxation time for protons in neutral fluoranthene exceeds 500 s and the relaxation via anion rotation is negligible in the metallic regime,[4] it is evident that the ^{13}C relaxation times are caused by hyperfine interactions with the conduction electrons.

IV. DISCUSSION

For the measured Knight-shift data (Table I) hyperfine interaction parameters can be easily evaluated with the help of Eq. (8) and the known paramagnetic susceptibility.[24,25] We use here the isotropic value $\chi_x = 1.06 \times 10^{-4}$ emu/mole since no anisotropy was observed in Ref. 25. Both isotropic and anisotropic hyperfine interactions are collected in Table II. Note that the hyperfine interaction is locally resolved and is related to the probability for finding a conduction electron at a particular site. This is called the "local spin density." Note that this simple picture is only correct for π electrons.

However, the relation between the local hyperfine interaction and the local spin density is by no means straightforward as was pointed out in Sec. II. In earlier work[7] we have used the Karplus-Fraenkel relation Eq. (11) (Ref. 11), which takes into account the core polarization due to on-site as well as neighboring-site spin density. Note that the negative sign of Q_n in Eq. (11) leads to possibly considerable negative hyperfine interaction even with positive spin density. This is in fact observed in our spectra for lines *g* and *h* which show large negative Knight shifts.

For a given spin-density distribution it might be useful to calculate the local isotropic hyperfine interaction by using Eq. (11). However, it is dangerous to derive the local spin density from a given data set of hyperfine interactions by a self-consistent solution of Eq. (11). In order to demonstrate this, we have included the spin densities calculated in this manner in column 3 of Table II. Note that the values are unreasonable and deviate strongly from the theoretical values.[7,33] Moreover, the sum over all local spin densities is negative. The failure of the Karplus-Fraenkel relation in $(FA)_2X$-type conductors may be connected with the fact that the bond length within the FA molecule varies considerably.[1]

As a more direct approach we propose here to use the dipolar part of the hyperfine interactions which were determined experimentally and are listed in Table II. Experimentally, only the Knight-shift component K_{33} and the total-shift tensor elements δ_{11}, δ_{22}, and δ_{33} are known. One therefore has to make an intelligent guess about the other Knight-shift components K_{11} and K_{22}. Figure 5 shows that the difference $\delta_{11}-\delta_{22}$ at the secondary carbon atoms has just the same value as the corresponding value of the chemical-shift differences in solid benzene. This means that $K_{11} \simeq K_{22}$; i.e., the Knight-shift tensor is effectively axially symmetric as is the corresponding hyperfine tensor. An axially symmetric hyperfine tensor is, in fact, expected due to the dipole interaction of the electron spin in the p_z orbital at the nuclear site.[34] This follows from symmetry considerations applied to Eq. (12). A contribution of spin densities at neighboring sites as well as spin polarizations of σ bonds should lead to a deviation from axial symmetry which can, however, not be severe as shown above. We conclude that their influence is less important.

TABLE II. Hyperfine tensor, i.e., isotropic part a and dipolar parts $A'_{33} = A_{33} - a$ and $(A'_{11} + A'_{22})/2 = (a - A_{33})/2$. The experimentally determined spin densities ρ_{iso} and ρ_{dip}, derived from these hyperfine interactions as described in the text are compared with the calculated spin densities ρ_{MO} according to a McLachlan-Hückel type MO theory (Refs. 7 and 33).

Site	a	ρ_{iso}	A'_{33}	$(A'_{11})+A'_{22})/2$	ρ_{dip}	ρ_{MO}
1	−4.03 MHz	−0.143	−0.48 MHz	0.24 MHz	0.002	−0.012
2	−5.45 MHz	−0.107	−3.36 MHz	1.68 MHz	−0.011	−0.011
3	7.29 MHz	0.024	13.49 MHz	−6.75 MHz	0.061	0.066
4	−2.05 MHz	−0.019	2.50 MHz	−1.25 MHz	0.015	0.024
5	0.81 MHz	−0.019	7.09 MHz	−3.55 MHz	0.035	0.025
6	6.35 MHz	−0.052	14.21 MHz	−7.10 MHz	0.066	0.065
7	−4.06 MHz	−0.114	−1.37 MHz	0.68 MHz	−0.002	−0.011
8	6.16 MHz	0.019	12.47 MHz	−6.24 MHz	0.057	0.067
9	−0.41 MHz	0.006	4.48 MHz	−2.24 MHz	0.023	0.026

We determine the pure dipolar part $A'_{33} = A_{33} - a_{iso}$ of the hyperfine interaction from K_{33} by using Eq. (8) and the known susceptibility. In a first approximation A'_{33} is directly proportional to the p_z spin density on the corresponding carbon atom. For absolute values of the spin densities we used the normalization of the spin density to one over the $(FA)_2^+$ dimer rather than an anisotropic coupling constant from the literature.[34] This seems to be justified in the light of no observed hyperfine interaction on the anions.[4,5] The total sum of A'_{33} over the $(FA)_2^+$ dimer was ascertained to be 204 MHz. This compares reasonably well with the theoretical value of 182 MHz from LCAO-MO calculations.[35]

In a second step we treat the effect of the spin densities in neighboring positions as a small perturbation. Within a point, dipole approximation A'_{33} can be calculated by a formula similar to Eq. (11) where the on-site normalized hyperfine constant $Q = 204$ MHz and the nearest-neighbor hyperfine constant $Q_n = -7$ MHz. The latter value demonstrates the minute influence of the neighboring sites.

The p_z spin densities obtained by this procedure are summarized in the sixth column of Table II. For a pictorial representation of the experimentally determined spin densities, we have plotted in Fig. 7 different circles where the circle diameter corresponds to the local spin density. It is evident from Table II that our experimental values agree surprisingly well with theoretical spin-density calculations based on a Hückel-McLachlan-MO theory.[7,33]

Finally, we want to discuss the relative size of the chemical-shift and Knight-shift tensor. The chemical-shift tensor at each nuclear site can be calculated from the difference between the total-shift and the Knight-shift values given in Table I. It turns out that the chemical-shift tensor for most sites is indeed very similar to the benzene chemical-shift tensor, as is expected for an aromatic molecule. It is dominated by the ordinary diamagnetic and paramagnetic contributions according to Eq. (4). The "Van Vleck contribution" Eq. (5) seems to be negligible, as was discussed above. The chemical-shift tensor is of the same order of magnitude at the different nuclear sites, whereas the Knight-shift tensor varies drastically for different positions according to the local distribution of the conduction electrons. Its magnitude is mostly smaller than the chemical-shift tensor except for those sites where the conduction-electron density is high. Interestingly enough, there the Knight-shift tensor is about as large as the chemical-shift tensor but with opposite sign. This leads to an almost complete cancellation of the total-shift anisotropy. The isotropic appearance of lines a,b,c is therefore accidental and buries, in fact, a large chemical as well as Knight-shift anisotropy.

V. SUMMARY

We have determined the locally resolved ^{13}C Knight-shift tensor in $(FA)_2X$ type organic conductors. From these data isotropic and anisotropic hyperfine interactions were determined at each particular carbon site. It was demonstrated that an uncritical application of the Karplus-Fraenkel relation for the determination of spin densities from hyperfine interactions may lead to unreasonable results. Spin densities from Knight-shift anisotropies, however, seem to be much more reliable due to the local nature of the dipole interaction. It can be concluded that a small or even negative p_z spin density at a specific site leads to a more or less isotropic Knight shift with a considerable negative value due to the spin density on neighboring atoms. A large p_z spin density results in a positive Knight shift with an important anisotropic part. The spin densities determined on this basis compare very well with a Hückel-McLachlan-MO calculation. These findings demonstrate once again that the conduction-band molecular orbital is largely determined by the molecular orbitals of the constituent molecules and not so much by the p_z overlap to neighboring molecules in the organic conductor. It seems to be, therefore, not surprising that the molecular packing in the solid occurs in such a way that the overlap between neighboring molecules is optimized at the position of highest spin density. A detailed spin-density map of the conduction electrons was obtained.

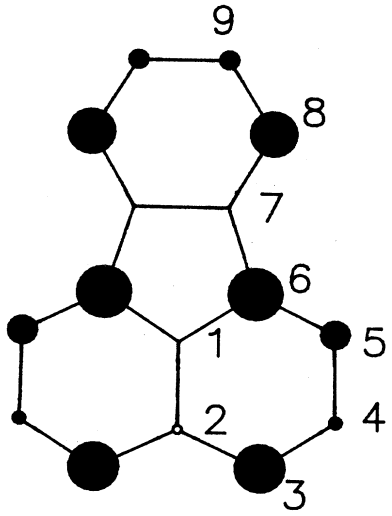

FIG. 7. Graphical representation of the local p_z-spin densities determined by the ^{13}C Knight-shift anisotropy. The diameter of the circles is proportional to the spin density; the open circles denote negative spin densities.

ACKNOWLEDGMENTS

We would like to thank U. Rempel for his collaboration in the temperature-dependent single-crystal experiments. We further thank Mrs. Ziliox and the Bruker company for the help with the temperature-dependent magic-angle-spinning experiments. We are grateful to Mrs. Grupp for the growth of the $(FA)_2PF_6$ single crystals. We also acknowledge valuable discussions with D. Jérôme, P. Bernier, P. C. Stein, C. Bourbonnais, C. Berthier, and H. Alloul. The Deutsche Forschungsgemeinschaft (DFG) has given financial support.

*Present address: Laboratoire de Physique des Solides, Universite Paris-Sud, F-91405 Orsay, France.

[1]V. Enkelmann, B. S. Morra, C. Kröhnke, and G. Wegner, Chem. Phys. **66**, 303 (1982).

[2]W. Stöcklein, B. Bail, M. Schwoerer, D. Singel, and W. Schmidt, in *Organic Molecular Aggregates,* edited by P. Reineker *et al.* (Springer-Verlag, Berlin, 1983), p. 228.

[3]G. G. Maresch, A. Grupp, M. Mehring, J. U. v. Schütz, and H. C. Wolf, J. Phys. (Paris) **46**, 461 (1985).

[4]W. Höptner, M. Mehring, J. U. v. Schütz, H. C. Wolf, B. S. Morra, V. Enkelmann, and G. Wegner, Chem. Phys. **73**, 253 (1982).

[5]W. Stöcklein and G. Denninger, Mol. Cryst. Liq. Cryst. **136**, 335 (1986).

[6]M. Mehring and J. Spengler, Phys. Rev. Lett. **53**, 2441 (1984).

[7]M. Mehring, M. Helmle, D. Köngeter, G. G. Maresch, and S. Demuth, Synth. Met. **19**, 349 (1987).

[8]F. Hentsch, M. Helmle, D. Köngeter, and M. Mehring, Phys. Rev. B **37**, 7205 (1988).

[9]J. Wieland, U. Haeberlen, D. Schweitzer, and H. J. Keller, Synth. Met. **19**, 393 (1987).

[10]P. Bernier, M. Audenaert, R. J. Schweizer, P. C. Stein, D. Jerome, K. Bechgaard, and A. Moradpour, J. Phys. (Paris) Lett. **46**, L675 (1985).

[11]M. Karplus and G. K. Fraenkel, J. Chem. Phys. **35**, 1312 (1961).

[12]P. Bernier, P. C. Stein, and C. Lenoir, Physica **143B**, 494 (1986).

[13]P. C. Stein, P. Bernier, and C. Lenoir, Phys. Rev. B **35**, 4389 (1987).

[14]A. M. Vajnrub, I. A. Khejnmaa, and E. B. Yagubskij, Pis'ma Zh. Eksp. Teor. Fiz. **44**, 247 (1986) [JETP Lett. **44**, 317 (1986)].

[15]W. Stöcklein, H. Seidel, D. Singel, R. D. Kendrick, and C. S. Yannoni, Chem. Phys. Lett. **141**, 277 (1987).

[16]G. Denninger, E. Dormann, M. Schwoerer, Synth. Met. **19**, 355 (1987).

[17]A. Abragam, *Principles of Nuclear Magnetism* (Oxford University Press, New York, 1961).

[18]W. D. Knight, Phys. Rev. **76**, 1259 (1949).

[19]V. Jaccarino, in *Theory of Magnetism in Transition Metals,* Proceedings of the International School of Physics, "Enrico Fermi," Course XXXVII, Varenna, 1966, edited by W. Marshall (Academic, New York, 1967), p. 335.

[20]J. A. Pople and D. L. Beveridge, *Approximate Molecular Orbital Theory* (McGraw Hill, New York, 1970).

[21]L. Ernst, Org. Magn. Reson. **8**, 161 (1976).

[22]M. Mehring, in *Low Dimensional Conductors and Superconductors,* Vol. 155 of *NATO Advanced Study Institute, Series B: Physics,* edited by D. Jerome and L. G. Caron (Plenum, New York, 1987), p. 185.

[23]R. A. Wind, H. Lock, and M. Mehring, Chem. Phys. Lett. **141**, 283 (1987).

[24]E. Dormann and U. Köbler, Solid State Comm. **54**, 1003 (1985).

[25]U. Köbler, J. Gmeiner, and E. Dormann, J. Magn. Magn. Mater. **69**, 189 (1987).

[26]C. Kröhnke, V. Enkelmann, and G. Wegner, Angew. Chemie **92**, 941 (1980).

[27]M. Mehring, *High Resolution NMR in Solids* (Springer-Verlag, Berlin, 1983).

[28]J. Herzfeld and A. E. Berger, J. Chem. Phys. **73**, 6021 (1980).

[29]M. Linder, A. Höhener, and R. R. Ernst, J. Magn. Res. **35**, 379 (1979).

[30]S. Pausak, A. Pines, and J. S. Waugh, J. Chem. Phys. **59**, 591 (1973).

[31]S. J. Opella and M. H. Frey, J. Am. Chem. Soc. **101**, 5854 (1979).

[32]D. Köngeter, doctoral thesis, University of Stuttgart, 1988; U. Rempel (unpublished).

[33]M. Helmle (private communication).

[34]T. Cole and C. Heller, J. Chem. Phys. **34**, 1085 (1961).

[35]J. R. Morton, Chem. Rev. **64**, 453 (1964).